Green Chemistry

PAPER

Cite this: *Green Chem.*, 2016, **18**, 2005

# Recovery of scandium from leachates of Greek bauxite residue by adsorption on functionalized chitosan–silica hybrid materials†

Joris Roosen,[a,c] Stijn Van Roosendael,[a] Chenna Rao Borra,[b] Tom Van Gerven,[b] Steven Mullens[c] and Koen Binnemans*[a]

Bauxite residue (red mud) is a waste residue that results from the production of alumina by the Bayer process. Since it has no large-scale industrial application, it is stockpiled in large reservoirs. Nevertheless, it should be considered as a valuable secondary resource as it contains relatively large concentrations of critical metals like the rare earths, scandium being the most important one. In this work, we investigated the recovery of scandium from real leachates of Greek bauxite residue. In the separation of scandium from the other elements, the biggest challenge arose from the chemical similarities between scandium(III) and iron(III). This hampers high selectivity for scandium, especially because iron, as one of the major elements in bauxite residue, is present in much higher concentrations than scandium. In order to achieve selectivity for scandium, chitosan–silica particles were functionalized with the chelating ligands diethylenetriamine pentaacetic acid (DTPA) and ethyleneglycol tetraacetic acid (EGTA). Both organic ligands were chosen because of the high stability constants between scandium(III) and the corresponding functional groups. The adsorption kinetics and the influence of pH on hydrolysis and adsorption were investigated batchwise from single-element solutions of scandium(III) and iron(III). In binary solutions of scandium(III) and iron(III), it was observed that only EGTA-functionalized chitosan–silica appeared to be highly selective for scandium(III) over iron(III). EGTA–chitosan–silica shows a much higher selectivity over state-of-the-art adsorbents for the separation of scandium(III) from iron(III). The latter material was therefore used as a resin material for column chromatography in order to effectively separate scandium from bauxite residue. Full separation was achieved by eluting the column with $HNO_3$ solution at pH 0.50; at this pH all other elements had already eluted.

Received 17th September 2015,
Accepted 9th November 2015

DOI: 10.1039/c5gc02225h

www.rsc.org/greenchem

## Introduction

The recovery of valuable metals from (industrial process) residues would be beneficial for both economical and sustainability reasons.[1–5] Especially, the production of rare-earth elements from secondary resources has gained interest as an additional route to their primary mining, since rare-earth elements have become indispensable in many modern high-tech and green applications.[1,6,7] Bauxite residue, also called "red mud", is the waste product of the production of alumina from bauxite by the Bayer process.[8] Bauxite residue is stockpiled in huge amounts, but it is harmful, mainly due to its high alkalinity (pH ≥ 12).[9–11] Besides its major components (iron oxides, quartz, sodium aluminosilicates, calcium carbonate/aluminate and titanium dioxide), bauxite residue also contains valuable minor elements, such as the rare earths. The concentrations of these metals are low, but with a production rate of 120 million tons per year, bauxite residue can be considered as an important candidate for valorization.[1] Moreover, compared to average concentration levels in the Earth's crust, bauxite residue is especially enriched in scandium. Scandium is mainly used in Al–Sc alloys, resulting in superior properties, such as light weight, high strength, good thermal resistance and long durability.[12] Another important application includes solid oxide fuel cells in which scandia-stabilized zirconia shows extremely high oxygen-ion conductivity for use as a highly efficient electrolyte.[13]

[a]*KU Leuven, Department of Chemistry, 3001 Heverlee, Belgium.*
*E-mail: Koen.Binnemans@chem.kuleuven.be; Tel: +32 16 32 74 46*
[b]*KU Leuven, Department of Chemical Engineering, 3001 Heverlee, Belgium*
[c]*VITO, Sustainable Materials Management, 2400 Mol, Belgium*

† Electronic supplementary information (ESI) available: Detailed synthesis procedures and IR-spectra. See DOI: 10.1039/c5gc02225h

To recover scandium and other rare earths from bauxite residue, they must be dissolved by leaching with inorganic acids. This is extensively investigated.[14–17] As a consequence of the high liquid-to-solid ratios generally used to obtain good recovery, the resulting leachate solutions contain low concentrations of scandium.[14] The most suitable technique for the concentration of very diluted scandium is therefore ion-exchange adsorption, which makes it possible to selectively recover scandium from the leachate by using appropriate types of ion-exchange resins, chelating resins, or varying desorption conditions.[15] Previous work shows that chitosan is a perfect material for the recovery of metal ions from diluted solutions using ion-exchange adsorption.[18,19] Chitosan is a linear polysaccharide which is mainly obtained by alkaline deacetylation of chitin, a naturally abundant material that can be found in the exo-skeleton of crustacea (such as lobsters and shrimps) and insects.[20–22] Its low cost, abundant availability, biocompatibility, biodegradability, non-toxicity, and convenient modification possibilities (both physically and chemically) make chitosan an interesting material for various applications, including the recovery of metals from aqueous solutions.[20–25] Chitosan shows excellent adsorption characteristics because of its high hydrophilicity (hydroxyl groups), high activity for the chelation of metal ions (primary amino groups), and a flexible structure which enables it to adopt a suitable configuration for complexation with metal ions.[26] The large number of highly reactive amino and hydroxyl groups allows for convenient modifications of the structure. In this way, selectivity for specifically targeted metal ions can be adjusted by the immobilization of an appropriate functional group.[26,27] Since pure chitosan suffers from poor mechanical properties and low porosity, it can be hybridized with silica to obtain organic–silica hybrid materials that combine the functional properties of the biopolymer with the stability and porosity of silica.[19,28,29] Functionalized chitosan–silica sorbents are useful as the stationary phase in chromatographic separation columns.[19,27,28]

In this paper, chitosan–silica hybrid materials were synthesized and functionalized with diethylenetriamine pentaacetic acid (DTPA) and ethyleneglycol tetraacetic acid (EGTA). The selectivity for the uptake of scandium(III) from nitrate leachates was investigated in binary, equimolar solutions of scandium(III) and iron(III) with respect to the functional group immobilized on the polymer matrix. The effective separation of scandium from the bauxite residue leachate was achieved in a column chromatography set-up with EGTA–chitosan–silica as the resin material and by eluting the loaded column with solutions with an increasing $HNO_3$ gradient (decreasing pH).

# Experimental

## Chemicals

Tetraethyl orthosilicate (TEOS, ≥99.0% pure) was purchased from Merck KGaA (Darmstadt, Germany). Chitosan (≥99.0% pure) was purchased from Sigma-Aldrich (Diegem, Belgium). $Fe(NO_3)_3{\cdot}9H_2O$ (≥99.0% pure) was purchased from J.T. Baker Chemicals B.V. (Deventer, The Netherlands). $Sc(NO_3)_3{\cdot}xH_2O$ (99.99% pure) was kindly supplied by Stanford Materials Corporation (Irvine, California, USA). Hydrochloric acid (37%), ethanol (99.99%) and sodium sulfite anhydrous (analytical reagent grade) were purchased from Fischer Scientific U.K (Loughborough, UK). Ammonia (25 wt%), *n*-heptane (99+%), nitric acid (65+%), gallium standard (1000 μg $mL^{-1}$ ± 0.4%), lanthanum standard (1000 μg $mL^{-1}$ ± 0.3%), cerium standard (1000 μg $mL^{-1}$ ± 2 μg) and holmium standard (1000 μg $mL^{-1}$ ± 0.4%) were purchased from Chem-Lab NV (Zedelgem, Belgium). Serva silicon solution was purchased from SERVA Electophoresis GmbH (Heidelberg, Germany). Acetic acid (100%) and sodium hydroxide (min 97.0%) were purchased from VWR International (Heverlee, Belgium). Pyridine (99+%), methanol (99.99%), acetic acid anhydride (99+%), sulfuric acid (96%) and diethylenetriamine pentaacetic acid (DTPA, 98+%) were purchased from Acros Organics (Geel, Belgium). Ethyleneglycol tetraacetic acid (EGTA, ultrapure grade; 97.0%) was purchased from Amresco Inc (Solon, Ohio, USA). *N*-(3-Dimethylaminopropyl)-*N*′-ethylcarbodiimide hydrochloride (EDC, 99%) was purchased from Fluorochem (Hadfield, UK). Bauxite residue, the precursor of the red mud leachates which have been studied in this work, was provided by the Aluminum of Greece Company, which is located at Agios Nikolaos, Greece. All products were used as received, without further purification.

## Equipment and analysis

FTIR spectra were recorded on a Bruker Vertex 70 spectrometer (Bruker Optics). Samples were examined as such using a Platinum ATR single reflection diamond attenuated total reflection (ATR) accessory. CHN (carbon, hydrogen, nitrogen) elemental analyses were obtained with the aid of a CE Instruments EA-1110 element analyser. Metal ion concentrations were determined by means of total-reflection X-ray fluorescence (TXRF) on a Bruker S2 Picofox TXRF spectrometer. To perform the sample preparation for a TXRF measurement, the unknown metal ion solution (900 μL) is mixed in an Eppendorf tube with a 1000 mg $L^{-1}$ gallium standard solution (100 μL) and stirred. A small amount of this prepared solution (5 μL) is put on a small quartz plate, pre-coated with a hydrophobic silicone solution (about 10 μL), and dried in an oven at 60 °C. Quantification of the metal ion concentration is derived from the absolute, known concentration of the gallium standard element and the signal ratio of the metal of interest and the gallium standard. Centrifugation was done by means of a Heraeus Megafuge 1.0 centrifuge. The MPLC chromatography separation set-up was composed of a Büchi chromatography pump B-688, to control the pressure and the eluent flow, and a glass Büchi BOROSILIKAT 3.3 column tube, no 17988 with dimensions of 9.6 mm × 115 mm (bed volume = 8.3 mL). The separated compounds were collected with the aid of a Büchi Automatic Fraction Collector B-684. The distinct fractions were monitored using *ex situ* analysis of the fractions with Inductively Coupled Plasma Mass Spectrometry (ICP-MS, Thermo Electron X Series).

 

## Methods

Chitosan–silica hybrid materials were made according to the *in situ* Stöber based method as described previously.[19] In this work, consecutive functionalization with DTPA from its anhydride was also described. The immobilization of EGTA proceeded differently, according to the method described by Zhao *et al.*[30] In this procedure, EGTA and chitosan–silica were combined with 1-ethyl-3-(3-dimethylaminopropyl) carbodiimide (EDC) at 40 °C. EDC is a water soluble cross-linking agent that activates carboxyl groups for the coupling of primary amines.[31] The leaching of bauxite residue was carried out by constant agitation for 24 h at 160 rpm and 25 °C. The leaching experiments were carried out with a 0.20 N $HNO_3$ solution with a liquid-to-solid ratio of 50 : 1.[14] The elemental composition of the native bauxite residue leachate is presented in Table 1. Note the low concentration of scandium in comparison with the concentrations of the major elements. The leachates were filtrated to remove solid particles.

Adsorption experiments were conducted by adsorption in batch mode, in aliquots of an appropriately diluted stock solution. Stock solutions were kept at pH 1.00. To adjust the experimental pH, 1.0 M HCl or 0.1 M NaOH was added to decrease or increase the pH, respectively. Functionalized particles were then weighed and added to the vials. Solutions were stirred at room temperature with a magnetic stirring bar at 300 rpm for 4 h. Next, the particles were separated from the aqueous solution by filtration, making use of a regenerated cellulose syringe filter with a pore size of 0.45 μm. The remaining metal ion concentration of the aqueous solution was measured using TXRF. The amount of metal ions adsorbed onto the chitosan–silica particles was then determined using the following formula:

$$q_e = \frac{(c_i - c_e)V}{m_{ads}} \quad (1)$$

In this formula, $q_e$ is the amount of adsorbed metal ions at equilibrium (mmol $g^{-1}$ adsorbent), $c_i$ is the initial metal ion concentration in aqueous solution (mmol $L^{-1}$), $c_e$ is the equilibrium metal ion concentration in aqueous solution (mmol $L^{-1}$), $V$ is the volume of the solution (0.010 L) and $m_{ads}$ is the mass of the adsorbent (0.025 g).

Column experiments were performed with the leachate of Greek bauxite residue. The column (bed volume = 8.3 mL) was packed with EGTA–chitosan–silica and connected to a chromatography pump to control the pressure (max. 10 bar) and the eluent flow. The experiments were preceded by thorough washing of the column with demineralized water, followed by conditioning of the column with a solution of $HNO_3$, set at pH 1.50 (the same as the leachate). After the addition of the sample to the column (10 mL), a decreasing pH gradient was applied with diluted solutions of $HNO_3$ in order to elute the coordinated ions from the column. The distinct fractions (5 mL) were monitored using *ex situ* analysis of the fractions with ICP-MS to determine the respective metal ion concentrations.

## Results and discussion

### Synthesis

DTPA–chitosan–silica and EGTA–chitosan–silica were successfully synthesized. The hypothesis was that the immobilization of these ligands on a matrix of chitosan–silica material would result in particles that show high selectivity for scandium. The immobilization of the functional groups proceeded by an amide reaction with the free available amino groups on the chitosan moieties of the hybrid particles. The resulting structure is shown in Fig. 1. Both sorbents appeared as white powders.

A summary of the characterization results (obtained mass, FT-IR and CHN) is given in Table 2. From these results, the hybridization and functionalization of the chitosan–silica matrix was confirmed. In the chitosan–silica hybrid materials, the ratio of organic : inorganic is approximately 1 : 4. By functionalization with organic ligands, the share of the organic component increases. From the respective values, it was concluded that the degree of functionalization was slightly higher for DTPA–chitosan–silica, compared to EGTA–chitosan–silica.

### Kinetics

The kinetics of scandium adsorption were investigated with DTPA–chitosan–silica and EGTA–chitosan–silica in single-

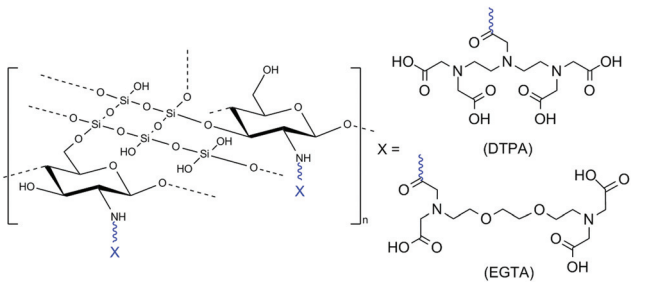


Fig. 1 Chemical structure of chitosan–silica, functionalized with DTPA or EGTA.

Table 1 Initial elemental composition of the native leachate of Greek bauxite residue. ∑Ln comprises all lanthanide elements (La, Ce, Pr, Nd, Sm, Eu, Gd, Tb, Dy, Ho, Er, Tm, Yb, and Lu)

| Element | Na | Ca | Al | Fe | Si | Ti | Sc | ∑Ln |
|---|---|---|---|---|---|---|---|---|
| Concentration (ppm) | 1104 | 939 | 670 | 106 | 558 | 106 | 2 | 6 |

Table 2 Summary of the characterization results for pure chitosan–silica, DTPA-functionalized chitosan–silica and EGTA-functionalized chitosan–silica

| Material | Mass yield (g) | Characteristic peak wavelengths ($cm^{-1}$) | Peak assignment | % C | % organic[a] |
|---|---|---|---|---|---|
| Chitosan–silica | 10.2 ± 0.8 | 3366 (broad band)<br>1559<br>1069 | O–H stretch + N–H stretch<br>C–N stretch<br>Si–O–Si symmetric stretch | 8.09 ± 0.06 | 20.1 |
| DTPA–chitosan–silica | 9.5 ± 0.5 | 3366 (broad band)<br>1636<br>1397<br>1065 | O–H stretch + N–H stretch<br>C═O stretch amide<br>Symmetric vibration $COO^-$<br>Si–O–Si symmetric stretch | 11.85 ± 0.21 | 29.5 |
| EGTA–chitosan–silica | 7.5 ± 0.5 | 3284 (broad band)<br>1636<br>1376<br>1071 | O–H stretch + N–H stretch<br>C═O stretch amide<br>Symmetric vibration $COO^-$<br>Si–O–Si symmetric stretch | 11.02 ± 0.06 | 27.4 |

[a] From the % C in the chitosan starting product (40.19%), an estimate can be made for the share of the organic component in the hybrid particles.

element nitrate solutions of scandium, with contact times ranging from 5 to 360 min (Fig. 2). Equilibrium was reached after 120 min, characterized by the beginning of a plateau in the adsorption curve. The plateau value corresponded, for DTPA–chitosan–silica, to an adsorption amount of 0.20 mmol Sc(III) per gram of sorbent material. This appears to be a low value, but corresponds to 100% recovery of the scandium ions present in the aqueous solution. The initial aqueous feed contains 0.50 mM of scandium ions, which approaches the low concentration of scandium in the diluted leachates of bauxite residue. For EGTA–chitosan–silica only 75% of the scandium present was adsorbed (0.15 mmol Sc(III) per gram of sorbent material). The lower adsorption amount for EGTA–chitosan–silica can be explained by the lower degree of functionalization, compared to that of DTPA–chitosan–silica (Table 2). Optimization of the synthesis procedure could improve this. In order to fully ensure equilibrium conditions before analyzing the residual concentration, all the following experiments were performed for an equilibration time of 240 min (4 h).

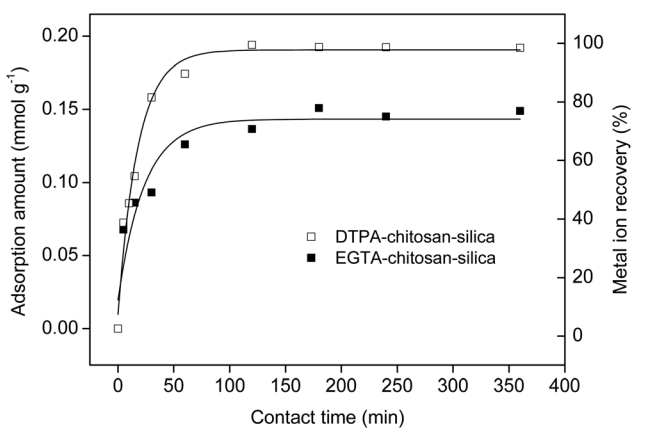


Fig. 2 Kinetics experiment. Sc(III) adsorption with DTPA–chitosan–silica and EGTA–chitosan–silica. Experimental conditions: $m_{ads}$ = 25.0 mg, $V$ = 10.0 mL, $c_{in}$ = 0.50 mM and $pH_{eq}$ = 2.02.

## Influence of pH

Adsorption was investigated as a function of the equilibrium pH. pH is an important parameter for adsorption, as it determines the protonation and deprotonation of the functional groups immobilized on the sorbent, and thus the mechanism of ion exchange and chelation. The influence of the equilibrium pH was investigated in single-element solutions of Sc(III) and Fe(III). In the first instance, only DTPA–chitosan–silica was considered (Fig. 3).

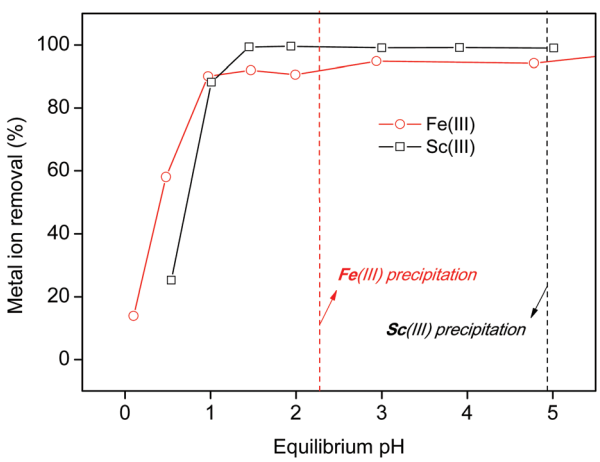


Fig. 3 Influence of the equilibrium pH on the removal of Fe(III) and Sc(III) ions from single-element solutions in the presence of DTPA–chitosan–silica. The vertical dashed lines indicate the respective pH values at which precipitation of Fe(III) and Sc(III) occurs because of hydrolysis. Experimental conditions: $m_{ads}$ = 25.0 mg, $V$ = 10.0 mL, $c_{in}$ = 0.50 mM and contact time = 4 h.

When interpreting these data, one has to pay attention to the fact that both metal ions are prone to hydrolysis. As a consequence, insoluble $Fe(OH)_3$ and $Sc(OH)_3$ compounds are formed when increasing the pH. Since the adsorption amount is in principle calculated from the residual concentration of the aqueous phase at equilibrium, one could make the wrong assumption that all metal ions removed from solution are effectively adsorbed. From the respective solubility product constants ($K_{sp}(Fe(OH)_3 = 2.79 \times 10^{-39}$, and $K_{sp}(Sc(OH)_3) = 2.22 \times 10^{-31}$)[32] and the metal ion concentration (0.50 mM), the pH at which precipitation occurs was calculated. This resulted in a value of 2.25 for Fe(III) and 4.88 for Sc(III). At higher pH values, one has to take into account precipitation as a phenomenon competing with adsorption in the removal of the corresponding metal ions from solution.

The main challenge for the isolation of pure scandium from the leachates of bauxite residue is to obtain selectivity for scandium especially compared to iron. Both elements behave chemically very similarly and it is therefore difficult to mutually separate them from a matrix of lots of other elements, like calcium, silicon and titanium. Moreover, the concentration of iron in the leachates from bauxite residue is usually much higher than that of scandium. From Fig. 3 it is evident that the affinity of DTPA–chitosan–silica is high for both Fe(III) and Sc(III). Both metal ions are (almost) fully adsorbed. We can assume that the metal ions are adsorbed because the plateau value is already reached at pH 1.50, which is below the pH range at which iron or scandium precipitates by hydrolysis reactions. It is further observed that the adsorption of Fe(III) starts at a lower pH in comparison with Sc(III). This indicates a higher affinity for Fe(III), compared to Sc(III).

### Hydrolysis

One could think of pH variation as a way to separate Fe(III) and Sc(III) since hydrolysis occurs at lower pH values for Fe(III) in comparison with Sc(III).[32] The precipitation of Fe(III) and Sc(III) was therefore investigated as a function of the equilibrium pH in an equimolar ($c_{aq}$ = 0.50 mM), binary solution of Fe(III) and Sc(III) (Fig. 4). Although significant precipitation (>50%) is observed for Fe(III) at lower pH values compared to Sc(III), we can also observe in Fig. 4 that the co-precipitation of scandium occurs.

Although at pH 3.50 almost four times more Fe(III) is precipitated compared to the amount of Sc(III), the 20% loss of scandium is not acceptable, taking into account its high economical value. Moreover, in the real leachates of bauxite residue, the relative amount of iron is significantly larger than that of scandium. It is therefore expected that also the amount of scandium co-precipitation would be significantly higher in real samples (if not 100%). This method was therefore not considered appropriate in the search for a method to isolate scandium efficiently from the leachates of bauxite residue. Also the possibilities of adding reducing agents (like zinc powder or sodium sulphite), or varying the counter anion (like sulphate or chloride) were investigated, but none of these methods were found to be useful. These observations only convinced us more of the hypothesis that an *intrinsically selective* adsorbent must provide scandium selectivity.

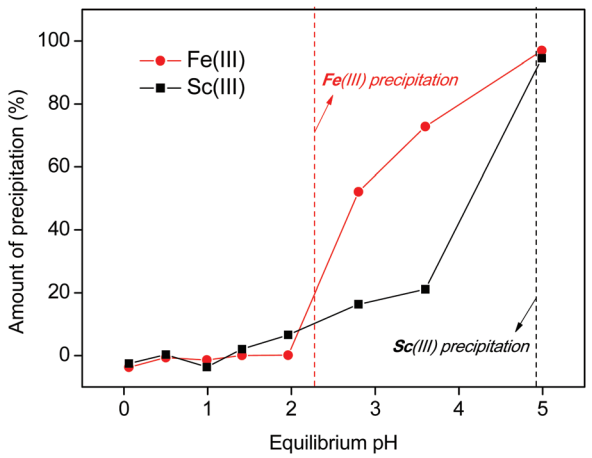


**Fig. 4** Investigation of $Fe(OH)_3$ and $Sc(OH)_3$ precipitation as a consequence of hydrolysis. The amount of precipitation is presented as a function of the equilibrium pH. The vertical dashed lines indicate the respective pH values at which the precipitation of Fe(III) and Sc(III) occurs because of hydrolysis. Experimental conditions: $V$ = 10.0 mL and $c_i$ = 0.50 mM.

### Selectivity experiment

The variation of the functional group immobilized on the chitosan–silica particles appeared to be a more successful strategy to obtain scandium selectivity. Since DTPA has already been proven to be a very efficient chelating molecule for rare earths, the functionalization of the chitosan–silica resin with DTPA groups was tested first in regards to its selectivity for scandium.[18] However, as was concluded from Fig. 3, the affinity of the DTPA-functionalized particles was higher for Fe(III) compared to Sc(III). This is a consequence of the corresponding stability constants between DTPA and Fe(III) or Sc(III), respectively (Table 3).

By closer inspection of different organic ligands and their corresponding stability constants with Sc(III) and Fe(III), one can see that EGTA has a remarkably higher affinity for Sc(III) compared to Fe(III), a difference of a factor of $10^5$ (Table 3). The

**Table 3** Stability constants (log $K$ values) for complexes formed between often used poly(amino) carboxylic ligands and the metal ions Fe(III), Sc(III) and Nd(III) (as a representative element for the lanthanides).[33]

| Organic ligand | Fe(III) | Sc(III) | Nd(III) |
|---|---|---|---|
| IDA[a] | 11.1 | 9.9 | 6.5 |
| NTA[b] | 15.9 | 12.7 | 11.3 |
| EDTA[c] | 25.1 | 23.1 | 16.6 |
| DTPA | 27.3 | 26.3 | 21.6 |
| EGTA | 20.5 | 25.4 | 16.3 |

[a] IDA = iminodiacetic acid. [b] NTA = nitrilotriacetic acid. [c] EDTA = ethylenediamine tetraacetic acid.

opposite is true for DTPA. Although DTPA has a high stability constant with Sc(III) ($\log K$ = 26.3), the stability constant with Fe(III) is even higher ($\log K$ = 27.3). To confirm the hypothesis that EGTA–chitosan–silica is more suited to separate Sc(III) from Fe(III) (and the other elements present in the leachate), the selectivity of both ligands was investigated in a binary solution of Fe(III) and Sc(III) ($c_{aq}$ = 0.50 mM for each metal ion). In Fig. 5, metal ion removal is presented as a function of the equilibrium pH for both DTPA–chitosan–silica (a) and EGTA–chitosan–silica (b), to be able to compare the adsorption behaviour of both sorbents. It becomes clear that the selectivity is reversed by switching from DTPA to EGTA as the chelating ligand. With EGTA–chitosan–silica, we are able to reach maximal adsorption for Sc(III) at pH 1.25, at which pH yet no Fe(III) is adsorbed at all. This high difference in selectivity is quite remarkable for two such chemically similar elements and could not be obtained with DTPA–chitosan–silica. Not only did DTPA–chitosan–silica show a higher affinity for Fe(III) compared to Sc(III), also the affinity profiles were much more similar. This is a consequence of the small difference (factor of 10) between the corresponding stability constants (Table 3).[33]

At pH 1.50 (Fig. 5b), no Fe(III) is adsorbed by EGTA–chitosan–silica, yet 80% of the Sc(III) ions are adsorbed from the aqueous solution. This remarkably higher affinity for scandium can be exploited in a column chromatography set-up to separate scandium from the other components present in a leachate of bauxite residue.

## Reusability

After adsorption of the metal ions from solution, the stripping of the immobilized ions is required for further processing and the regeneration of the sorbent. No concentrated acid or solutions of strongly chelating agents were necessary to desorb the strongly immobilized Sc(III) ions from EGTA–chitosan–silica. By simply contacting the loaded particles with $HNO_3$ solution, 100% stripping was observed for $HNO_3$ concentrations higher than 0.75 M. 1.00 M $HNO_3$ was used next in the reusability procedure to ensure full stripping. Reusability was investigated for EGTA–chitosan–silica by repeating the adsorption/desorption cycle seven times. The resulting adsorption values were each time compared with the adsorption amount in the first cycle to determine the adsorption efficiency (Fig. 6). The adsorption efficiency decreased by about 10% in the second adsorption cycle. This is probably due to partial hydrolysis of the immobilized EGTA groups by the acid used in the first stripping step. The residual capacity remained quite constant. After the 7$^{th}$ adsorption cycle, the adsorption efficiency was still 90%. The (minimal) decreases observed after the second cycle could more likely be attributed to physical losses because of the manual handling during consecutive adsorption/desorption cycles, rather than to physical or chemical damage to the par-

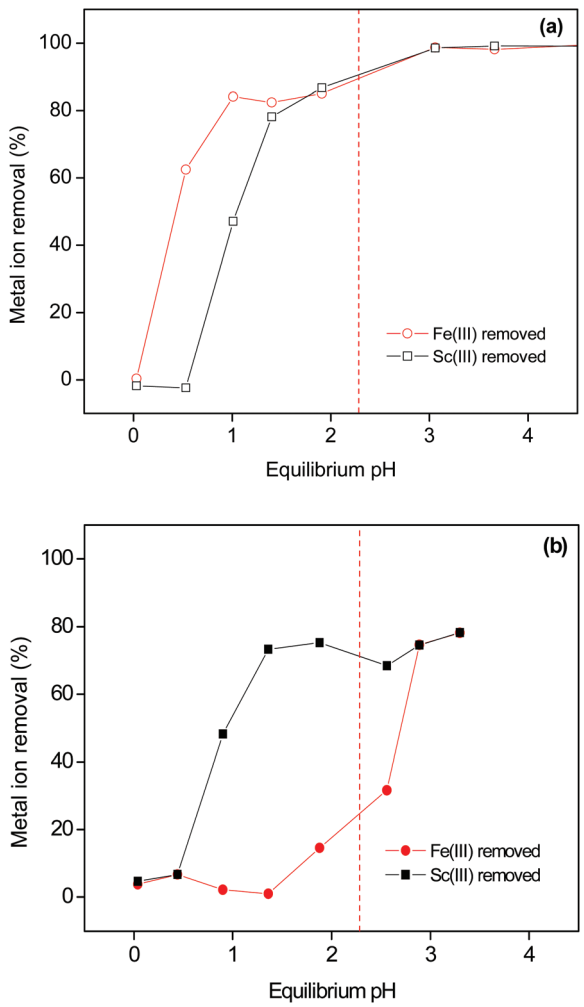


Fig. 5 Metal ion removal from a binary, equimolar solution of Fe(III) and Sc(III) in the presence of DTPA–chitosan–silica (a) or EGTA–chitosan–silica (b). The vertical dashed line indicates the pH at which the precipitation of Fe(III) occurs because of hydrolysis. Experimental conditions: $m_{ads}$ = 25.0 mg; $V$ = 10.0 mL; $c_i$ = 0.50 mM; adsorption time = 4 h.

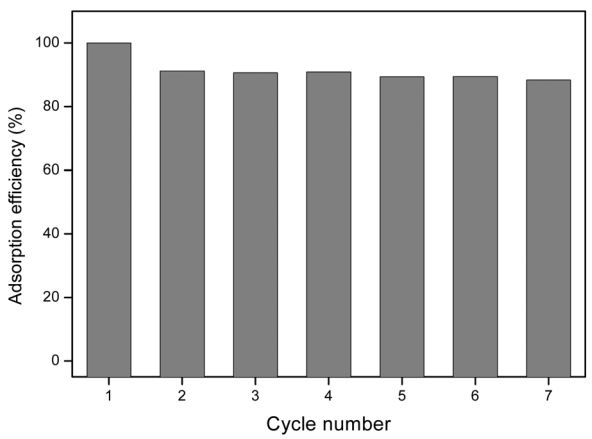


Fig. 6 Reusability of EGTA–chitosan–silica. Adsorption from an aqueous solution of $Sc(NO_3)_3$. Stripping with 1.0 M $HNO_3$ (10.0 mL). Experimental conditions: $m_{ads}$ = 25.0 mg; $V$ = 10.0 mL; $c_i$ = 0.50 mM; adsorption time = 4 h; stripping time = 1 h.

ticles because of the stripping treatment, as it is expected that all loosely bound EGTA-ligands have been hydrolyzed during the first stripping step.

### Column separation experiments

The higher the affinity of a given metal ion for a functionalized resin, the slower the migration through a chromatography column will be. The isolation of scandium was investigated using the principle of ion-exchange column chromatography with EGTA–chitosan–silica as the resin material in an MPLC-set-up. A bauxite residue leachate sample was added on top of the column, pre-equilibrated at a pH of 1.50, just like the leachate. Elution with aqueous solutions of $HNO_3$ (at a flow rate of 40 mL $h^{-1}$) then enabled the collection of distinct fractions of metal ions in the order of affinity for the resin material. A decreasing pH gradient was applied (from pH 2.00 to pH 0.00) in order to induce consecutive desorption of the distinct complexed metal ions. The resulting chromatogram (metal ion concentration as a function of elution volume) is presented in Fig. 7.

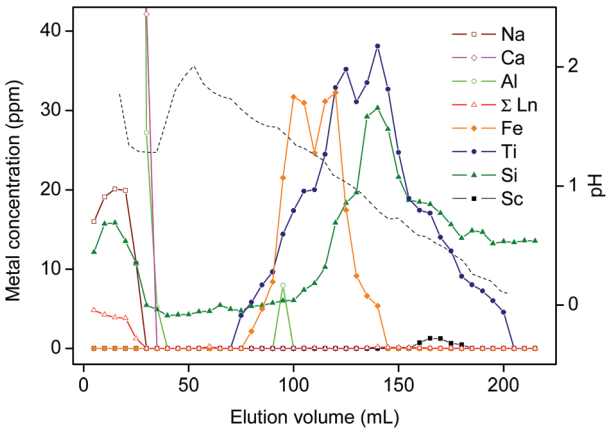


**Fig. 7** Chromatogram of scandium separation from a bauxite residue leachate using ion-exchange column chromatography with EGTA–chitosan–silica as the resin material and a decreasing pH gradient. The metal concentration is presented as a function of the elution volume. ∑Ln comprises all lanthanide elements (La, Ce, Pr, Nd, Sm, Eu, Gd, Tb, Dy, Ho, Er, Tm, Yb, and Lu). The dotted line represents the pH of the distinct fractions (right axis).

Peaks dropping after the first few fractions are explained by the fact that the pH gradient started from pH 2.00, while the column was set before at a lower pH of 1.50. Given the high affinity for Sc(III), it is observed that the peak of Sc(III) is located after 150 mL, corresponding to an elution pH of 0.50, at which most of the other elements have eluted already. Moreover, the big difference between scandium and the lanthanides is remarkable. However, the lower affinity of the resin for the lanthanides can be explained by the lower stability constant between EGTA and the lanthanides compared to scandium. Further, it has to be noted that the desorbed scandium fractions still contain titanium and silicon impurities. Nevertheless, the largest fractions of these ions eluted earlier. The highest breakthrough peaks of Ti(IV) and Si(IV) are situated around a pH value of 0.80. These observations indicate that an even better separation could be obtained by the optimization

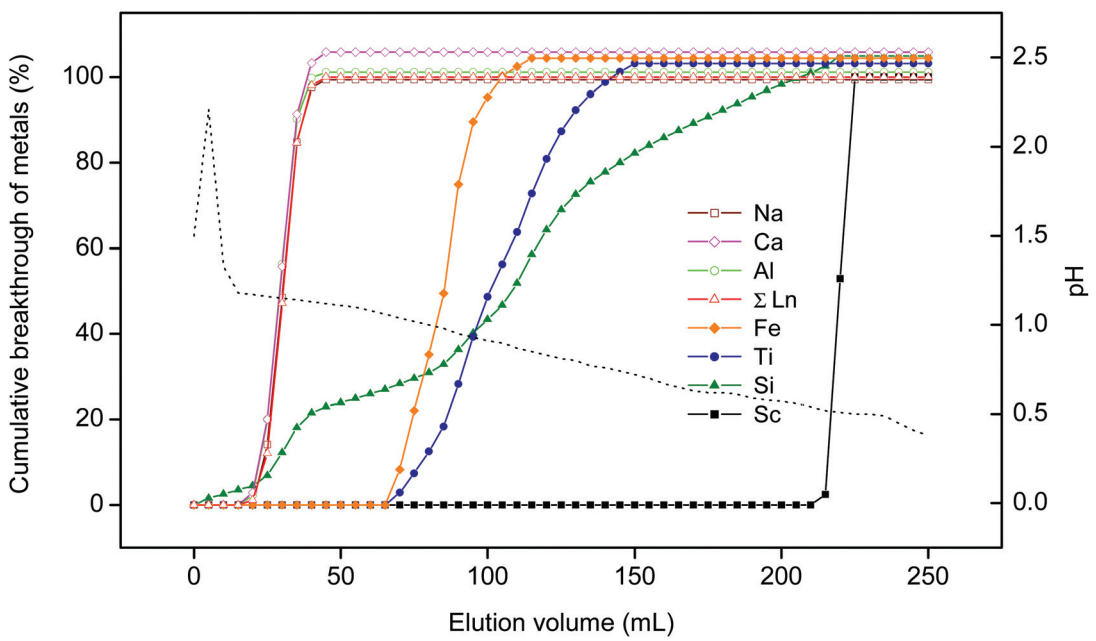


**Fig. 8** Optimized isolation of scandium from the bauxite residue leachate using ion-exchange column chromatography with EGTA–chitosan–silica as the resin material and a decreasing pH gradient. The cumulative breakthrough of the distinct metals is presented as a function of the elution volume. ∑Ln comprises all lanthanide elements (La, Ce, Pr, Nd, Sm, Eu, Gd, Tb, Dy, Ho, Er, Tm, Yb, and Lu). The dotted line represents the pH of the distinct fractions (right axis).

of the experimental conditions. Possibilities to improve the separation include a slower decreasing pH gradient, a lower flow rate, a longer column and the consideration of other types of eluents.

A second column experiment was performed by just changing the pH gradient and the flow rate (to 30 mL $h^{-1}$). The same column (with equal amounts of the same material) was used as in the first experiment. Elution was immediately started from pH 1.50 and more fractions were collected before eluting with pH 0.50 to strip off scandium from the column. The resulting chromatogram is presented in Fig. 8. In this figure, unlike Fig. 7, the breakthrough of the different metal ions is presented in a different way for the sake of clarity. To be able to compare the behaviour of scandium to the major elements (the latter being present in significantly higher concentrations in the leachate) the breakthrough is better presented as a percentage of the initial concentration, in a cumulative way (adding up from 0 to 100%) as a function of elution volume. A sudden pH increase is observed during column loading. This can probably be attributed to an increase of the ionic strength of the column.[34] Next to that, the effect of the experimental optimization becomes very clear from Fig. 8. By going faster to lower pH values, all elements, except for scandium, start to elute at lower elution volumes. Moreover, elution at pH values between 1.00 and 0.50 was maintained for a longer time. This allowed all the iron, titanium and silicon to fully elute from the column before scandium was stripped from the column at pH 0.50, in only two fractions. EGTA–chitosan–silica has such a high affinity for scandium, so that we managed to separate it from the real leachate of bauxite residue in only one simple chromatography cycle, with a high recovery rate (about 25 bed volumes). To the best of our knowledge, a higher selectivity for scandium has not been reported before. Both scandium fractions could then be combined and concentrated by evaporation for further processing.

## Conclusions

Functionalization of chitosan–silica particles with EGTA groups resulted in a hybrid material with an exceptionally high adsorption affinity for scandium, higher than that of a similar hybrid material functionalized with DTPA groups. The high selectivity for scandium was confirmed in equimolar, binary solutions of Sc(III) and Fe(III) and eventually exploited to separate scandium from other components (mainly iron, titanium and silicon) in a $HNO_3$ leachate of Greek bauxite residue. Scandium was isolated from the other elements using ion-exchange column chromatography, by applying a decreasing pH gradient with aqueous solutions of $HNO_3$. Scandium broke through the column at a pH of 0.50, a much lower value than the ones observed for the other metal ions present in the leachate. This allowed us to strip pure scandium fractions from the column with a high recovery rate.

## Acknowledgements

This work was funded by VITO, the Research Foundation – Flanders (FWO, PhD fellowship to JR) and KU Leuven (DBOF grant to CRB and IOF-KP RARE$^3$). The authors also wish to thank Aluminum of Greece for providing the bauxite residue sample. Michèle Vanroelen is thanked for performing the ICP measurements.

## Notes and references

1 K. Binnemans, P. T. Jones, B. Blanpain, T. Van Gerven and Y. Pontikes, *J. Cleaner Prod.*, 2015, **99**, 17–38.
2 Y. V. Nancharaiah, S. Venkata Mohan and P. N. L. Lens, *Bioresour. Technol.*, 2015, **195**, 102–114.
3 H. Dong, J. Zhao, J. Chen, Y. Wu and B. Li, *Int. J. Miner. Process*, 2015, DOI: 10.1016/j.minpro.2015.06.009.
4 Z. Shengqiang, H. Xiuyang and W. Dahui, *Rare Met. Mater. Eng.*, 2015, **44**, 73–78.
5 R. Banda, T. H. Nguyen, S. H. Sohn and M. S. Lee, *Hydrometallurgy*, 2013, **133**, 161–167.
6 S. Massari and M. Ruberti, *Resour. Policy*, 2013, **38**, 36–43.
7 K. Binnemans, P. T. Jones, B. Blanpain, T. Van Gerven, Y. Yang, A. Walton and M. Buchert, *J. Cleaner Prod.*, 2013, **51**, 1–22.
8 A. R. Hind, S. K. Bhargava and S. C. Grocott, *Colloids Surf., A*, 1999, **146**, 359–374.
9 G. Power, M. Gräfe and C. Klauber, *Hydrometallurgy*, 2011, **108**, 33–45.
10 C. Klauber, M. Gräfe and G. Power, *Hydrometallurgy*, 2011, **108**, 11–32.
11 M. Gräfe, G. Power and C. Klauber, *Hydrometallurgy*, 2011, **108**, 60–79.
12 Z. Ahmad, *JOM*, 2003, **35**, 35–39.
13 S. P. S. Badwal, F. T. Ciacchi and D. Milosevic, *Solid State Ionics*, 2000, **136–137**, 91–99.
14 C. R. Borra, Y. Pontikes, K. Binnemans and T. Van Gerven, *Miner. Eng.*, 2015, **76**, 20–27.
15 O. Petrakova, G. Klimentenok, A. Panov and S. Gorbachev, presented in part at the ERES2014: 1st European Rare Earth Resources Conference, Milos, 04-07/09/2014, 2014.
16 W. Wang, Y. Pranolo and C. Y. Cheng, *Hydrometallurgy*, 2011, **108**, 100–108.
17 M. T. Ochsenkühn-Petropoulou, K. S. Hatzilyberis, L. N. Mendrinos and C. E. Salmas, *Ind. Eng. Chem. Res.*, 2002, **41**, 5794–5801.
18 J. Roosen and K. Binnemans, *J. Mater. Chem. A*, 2014, **2**, 1530–1540.
19 J. Roosen, J. Spooren and K. Binnemans, *J. Mater. Chem. A*, 2014, **2**, 19415–19426.
20 E. Guibal, *Sep. Purif. Technol.*, 2004, **38**, 43–74.
21 N. Mati-Baouche, P.-H. Elchinger, H. de Baynast, G. Pierre, C. Delattre and P. Michaud, *Eur. Polym. J.*, 2014, **60**, 198–212.

 

22 A. J. Varma, S. V. Deshpande and J. F. Kennedy, *Carbohydr. Polym.*, 2004, **55**, 77–93.
23 S. E. Bailey, T. J. Olin, R. M. Bricka and D. D. Adrian, *Water Res.*, 1999, **33**, 2469–2479.
24 E. Guibal, C. Milot and J. M. Tobin, *Ind. Eng. Chem. Res.*, 1998, **37**, 1454–1463.
25 A. El Kadib, *ChemSusChem*, 2015, **8**, 217–244.
26 K. Inoue, K. Yoshizuka and K. Ohto, *Anal. Chim. Acta*, 1999, **388**, 209–218.
27 S. S. Rashidova, D. S. Shakarova, O. N. Ruzimuradov, D. T. Satubaldieva, S. V. Zalyalieva, O. A. Shpigun, V. P. Varlamov and B. D. Kabulov, *J. Chromatogr., B: Biomed. Appl.*, 2004, **800**, 49–53.
28 H. Zhao, J. Xu, W. Lan, T. Wang and G. Luo, *Chem. Eng. J.*, 2013, **229**, 82–89.
29 E. Repo, J. K. Warchol, A. Bhatnagar and M. E. T. Sillanpää, *J. Colloid Interface Sci.*, 2011, **358**, 261–267.
30 F. Zhao, E. Repo, D. Yin and M. E. Sillanpaa, *J. Colloid Interface Sci.*, 2013, **409**, 174–182.
31 S. K. Vashist, *Diagnostics*, 2012, **2**, 23–33.
32 *CRC Handbook of Chemistry and Physics*, CRC Press LLC, Boca Raton, USA, 2003–2004.
33 D. D. Perrin, *Stability Constants, Part B Organic Ligands*, Pergamon, Oxford, 1979.
34 C. D. Kennedy, *Biochem. Educ.*, 1990, **18**, 35–40.